Complexation of Gold Nanoparticles with Radiolytically Generated Thiocyanate Radicals ($(SCN)_2^{\bullet -}$)

Amy Dawson and Prashant V. Kamat*

Notre Dame Radiation Laboratory, University of Notre Dame, Notre Dame, Indiana 46556-0579

Received: August 24, 2000; In Final Form: October 30, 2000

Pulse radiolytically generated $(SCN)_2^{\bullet -}$ radicals bind strongly to the gold nanoparticle surface, with an apparent equilibrium constant of 4.7×10^3 M^{-1}. The resultant complex has a strong absorption band at 390 nm which quickly undergoes chemical changes to yield an oxidation product, $[Au(SCN)_2]^-$, with an absorption maximum at 320 nm. The spectral changes associated with the chemical interaction between SiO_2/Al_2O_3-stabilized gold nanoparticles and $(SCN)_2^{\bullet -}$ are elucidated using time-resolved transient absorption spectroscopy.

Introduction

Metal nanoclusters such as gold possess an unusual property of chemically binding with functional groups such as −SH, −CNS, $-NH_2$, etc. The chemical binding of these groups to a gold surface has important applications in designing nanoscale materials for biological nanosensors and optoelectronic nanodevices.[1−3] For example, the ability of the gold surface to bind with specific functional groups has made them suitable for biomolecular labeling.[3] Engineering of the nanocluster surfaces, with electro- or photoactive molecules, can provide three-dimensional molecular arrangements around the nanoparticles. Researchers have often used functional groups such as thiols, amines, or isothiocyanate to attach electroactive or photoactive molecules to the gold surface.[4−12] In a recent study,[13] we have used an amine-tethering group for organizing pyrene chromophores onto the gold nanoparticles. Surface binding of the amine group to the gold surface suppresses intramolecular charge transfer interactions with the pyrene chromophore, which in turn increases the efficiency of the radiative process of the excited chromophore by 30 times. Self-assembly of such fluoroprobes around gold nanocores can provide information about the microenvironments and aid in designing nanosized inorganic−organic hybrid materials that are soluble in organic solvents.

Binding of electronegative (or electropositive) groups to the gold surface often leads to dampening of the surface plasmon band of gold nanoparticles.[14,15] The influence of surrounding material on the damping of the surface plasmon band of the metal nanocluster has been extensively studied by Kreibig and co-workers.[16,17] Neutralization of surface charge caused by the surface binding of a chemical species often leads to aggregation effects.[9] The size- and shape-dependent optical properties of gold colloids have been reviewed recently.[18] Noble metals deposited on oxide surface often promote catalytic reactions (for example, Pt-deposited TiO_2 photocatalysts are used in water splitting reactions).[19,20] Colloidal gold aerogel materials have also been developed as advanced sensor, catalytic, and electrocatalytic materials.[21] Recently, Halas and co-workers[22−25] have investigated the effect of an oxide core on the optical properties of gold nanoshell and chemically bound gold nanoparticles.

* Address correspondence to this author. E-mail: pkamat@nd.edu. Web: http://www.nd.edu/~pkamat.

As the applied aspects of these surface modified metal nanoparticles become increasingly important, there is a need to understand the chemical interactions and the stability of these nanoassemblies toward reactive radicals. Pulse radiolysis has been found to be quite useful to elucidate the role of metal particles in many catalytic reactions.[26−31] To the best of our knowledge, no major effort has been made to probe the surface complexation of short-lived oxidizing radicals with gold nanoparticles. We report here for the first time the complexation of a mildly oxidizing radical, $(SCN)_2^{\bullet -}$, with gold nanoparticles in aqueous solution and the spectral changes associated with such a chemical interaction.

Experimental Section

Preparation of Al_2O_3/SiO_2/Au Colloids. Hydrogen tetrachloroaurate(III) and sodium thiocyanate, NaSCN, were obtained from Aldrich Chemical Co. and used as received. The alumina-capped silica (SiO_2/Al_2O_3) colloids (3.8 (w/w) % Al_2O_3 and 19 (w/w) % SiO_2, batch number 15J613) was obtained from Nalco Chemical Co. The particle diameter of SiO_2/Al_2O_3 colloids suspended in an aqueous solution (pH 4.5) was 20 nm. 20 mL of the 10 mM $HAuCl_4$ stock solution was added dropwise with vigorous stirring to 20 mL of water containing 2 mL of the SiO_2/Al_2O_3 colloidal solution. Sodium borohydride (8 mM) was then added dropwise until a color change from pale yellow to dark purple occurred. The transparent suspension of gold-capped SiO_2/Al_2O_3 colloids was stable enough to conduct transient absorption measurements. For pulse radiolysis experiments we added 20 mL of 0.5 M SCN^- dropwise to the colloidal suspension with stirring. Deionized water was added to bring the total volume to 200 mL. (Final concentrations were $[SiO_2/Al_2O_3] = 0.04$ M, [Au] = 1 mM, and $[SCN^-] = 0.05$ M.) A suspension of gold nanoparticles without the SiO_2/Al_2O_3 core was prepared by the thiocyanate reduction method.[32,33] These particles are too small (diameter 2 nm) to exhibit any surface plasmon absorption.

Transmission electron microscope (TEM) images were taken using a Hitachi H600 transmission electron microscope at a magnification factor of 200 000×. One drop of sample was placed on a carbon-coated copper grid for imaging and blotted to remove excess water.

Pulse Radiolysis. Pulse radiolysis experiments were performed using a model Titan Beta-8/16-1S LINAC. This LINAC

10.1021/jp0030490 CCC: $19.00
Published on Web 11/28/2000

SCHEME 1

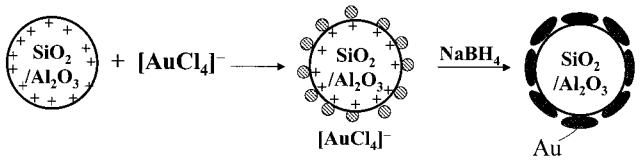

produces electron pulses, 50 ns in duration, at energy 8 MeV. The dose in pulse mode was determined to be approximately 6.0 Gy, based on the oxidation of thiocyanate (SCN^-) to $(SCN)_2^{\bullet-}$ in a N_2O-saturated solution. Solution was continuously flowed through a quartz cell during the pulse radiolysis experiment.

Results and Discussion

The borohydrate reduction method is a convenient technique to reduce noble metal ions in aqueous solution. Unlike the citrate reduction procedure,[34] the borohydrate reduction method requires a stabilizer to keep the reduced gold nanoparticles suspended uniformly in solution. Charged colloids and polymers are often used to stabilize such colloids in solution. For example, earlier attempts have shown that the metal oxide colloids such as SiO_2 can facilitate stabilization of the metal or semiconductor nanoparticles.[35−37] In the present study we have chosen alumina-capped silica (SiO_2/Al_2O_3) nanoparticles (particle diameter 20 nm) as the stabilizer since the positively charged oxide surface facilitates binding of $[AuCl_4]^-$ via electrostatic interactions. The net positive charge carried on the surface of these particles induces strong affinity to bind anions quantitatively.[38,39] Reduction of $[AuCl_4]^-$ with freshly prepared sodium borohydrate solution yields gold nanocluster deposits on SiO_2/Al_2O_3 nanoparticles (Scheme 1).

The SiO_2/Al_2O_3 nanoparticles act as a stabilizer by uniformly distributing $[AuCl_4]^-$ on the surface prior to reduction. The SiO_2/Al_2O_3-stabilized gold nanoparticles (referred as SiO_2/Al_2O_3/Au) show good dispersibility in aqueous solution without undergoing aggregation or precipitation. Lowering the support concentration below 1:1 molar ratio of the support and $[AuCl_4]^-$ causes precipitation of colloids. The necessity of the oxide support for achieving colloidal stabilization is an indirect indication that the gold nanoparticles are deposited onto the SiO_2/Al_2O_3 surface. It should be noted that the present methodology is slightly different than the one considered earlier[40] to deposit gold nanoshell onto silica nanoparticles. This method involved mixing of amine-functionalized silica particles with a solution of gold nanoparticles for directly attaching gold nanoparticles to silica. Lack of such binding groups in our experiments will result in a loosely bound layer of gold nanoclusters on SiO_2/Al_2O_3 core. It is likely that the gold capping formed on the SiO_2/Al_2O_3 nanoparticles is a discontinuous shell made up of several small gold nanoclusters or islands. Metijevic and co-workers[41−43] have shown that a variety of surface coatings can be produced on cores of very different compositions. They have shown that the formation of coatings on particles dispersed in liquids need not depend on specific interfacial reactions.

Figure 1A shows the electron micrograph of gold-capped SiO_2/Al_2O_3 nanoparticles deposited on a carbon-coated copper grid. The micrograph shows fairly well dispersed nanoparticles with a particle diameter of 15−25 nm. These particles have relatively thin gold shell with no significant change in particle size compared to the original SiO_2/Al_2O_3 core. Since we could not observe any separate smaller gold nanoparticles, we conclude that the gold deposition occurs over the surface of SiO_2/Al_2O_3

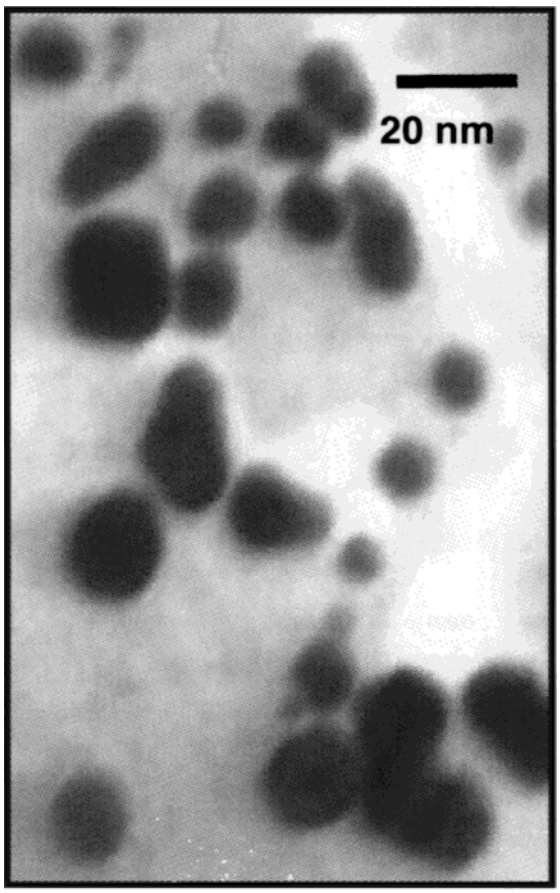

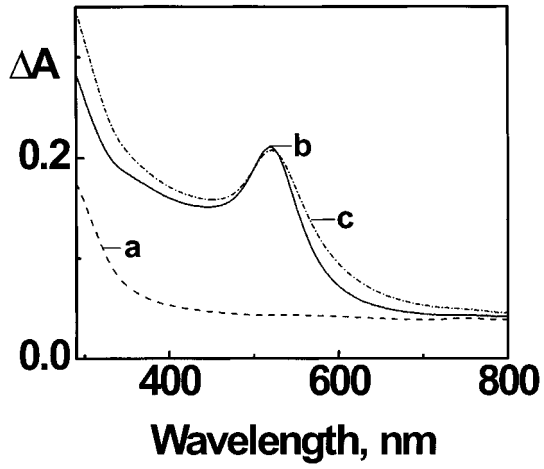

Figure 1. (A, top) Transmission electron micrograph of SiO_2/Al_2O_3/Au nanoparticles. (B, bottom) Absorption spectra of SiO_2/Al_2O_3 colloids (0.04 M) (a) before and (b) after reduction of $AuCl_4^-$ (1 mM). Spectrum (c) was recorded after the addition of NaSCN (0.05 M) to solution of (b).

nanoparticles. On the basis of the concentration of $AuCl_4^-$, we expect the gold layer thickness to be of the order of 2−3 nm. It should also be noted that these TEM studies do not provide a detailed information about the continuity or the uniformity of the gold layer. High-resolution TEM studies are necessary to further establish the nature of such shells.

The absorption spectra of these particles before and after the deposition of gold layer are shown in Figure 1B. The SiO_2/Al_2O_3-stabilized gold nanoparticles show characteristic surface plasmon absorption band at 530 nm. This absorption is similar to the one reported for larger size gold nanoparticles.[44] Small

dampening and broadening of this surface plasmon band is seen in the presence of SCN^-(spectrum c in Figure 1B). As shown earlier,[14,15] the surface plasmon absorption band of metal nanoclusters is very sensitive to the adsorbed ions. A more detailed discussion on the damping effects caused by surrounding material can be found elsewhere.[16,17,45]

The presence of silica core has been shown to affect the optical properties of metal nanoclusters.[17] Strong red shift and drastic broadening of the surface plasmon band were observed for Ag nanoclusters embedded in various dielectric oxides. Halas and co-workers[23,24] have shown that the presence of a dielectric core can induce dipolar plasmon resonances in the infrared. The optical absorption of silica core−gold shell nanostructures can be varied from 800 to 2200 nm by varying the relative size of the core and shell. It should be noted that these measurements were carried out with thin films consisting of silica cores coated with gold nanoshells and by excluding solvent medium. However, no such infrared absorption could be seen for the silica core−gold nanoshell[40] or gold core−silica nanoshell[5,12] particles suspended in aqueous medium. The spectral features of SiO_2/Al_2O_3/Au shown in Figure 1B do not indicate any significant red shift in the plasmon absorption or absorption bands in the infrared, thus ruling out direct interaction with the SiO_2/Al_2O_3 surface. Weak interaction between the SiO_2/Al_2O_3 and the gold layer, and the dominance of surrounding aqueous medium, are the possible reasons for not observing the influence of dielectric oxide core.

Radiolysis is a convenient technique to produce reductive and oxidative radicals in aqueous solutions. The primary products (e_{aq}^-, $^\bullet OH$, $H^\bullet$ etc.) produced during the radiolysis of water can be tuned to create controlled reductive or oxidative conditions. For example, we can achieve oxidative conditions through the purging of N_2O gas and scavenge aqueous electrons to yield a solution that exclusively produces hydroxyl radicals (reaction 1).

$$e_{aq} + N_2O + H_2O \rightarrow N_2 + {}^\bullet OH + OH^- \qquad (1)$$

The presence of high concentrations of SCN^- in N_2O-saturated aqueous solution results in the formation of the mildly oxidative thiocyanate radical that can further react with substrates present in solution via a diffusion-controlled process.

$$^\bullet OH + SCN^- \rightarrow SCN^\bullet + OH^- \xrightarrow{SCN^-} (SCN)_2^{\bullet -} \qquad (2)$$

Thus, we are able to probe the reactivity of $(SCN)_2^{\bullet -}$ toward the SiO_2/Al_2O_3-stabilized gold nanoparticles. This is investigated in a pulse radiolysis experiment by recording transient absorption−time profiles at different monitoring wavelengths.

The spectral changes following the generation of $(SCN)_2^{\bullet -}$ radicals in the pulse radiolysis of colloidal SiO_2/Al_2O_3/Au suspension in water (pH 4.5, N_2O saturated) containing 0.05 M NaSCN were also recorded. The time-resolved difference absorbance spectra recorded following the pulse radiolysis of Au-capped SiO_2/Al_2O_3/Au colloids and 0.05 M SCN^- are shown in Figure 2. The difference absorbance spectrum recorded immediately after the electron pulse shows an absorbance maximum at 480 nm, which is a characteristic absorption feature of $(SCN)_2^{\bullet -}$ radicals (reaction 2). However, the absorption at 480 nm quickly decays and a new absorption band at 390 nm appears. The transient absorption spectrum recorded 140 μs after the electron pulse irradiation shows the spectral changes that occur during the decay of $(SCN)_2^{\bullet -}$ radicals. The growth of the absorption at 390 nm parallels the absorption decay at 480 nm. A similar transient formation with maximum around 390 nm is also seen when gold colloids that were prepared without the SiO_2/Al_2O_3 core react with pulse radiolytically generated $(SCN)_2^{\bullet -}$ radicals (See Figures 1 and 2 in Supporting Information).

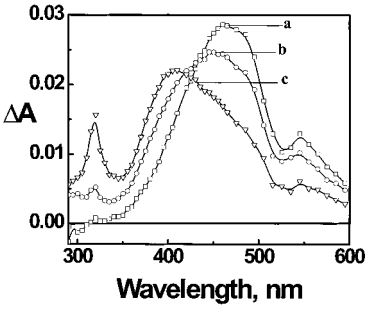

Figure 2. Transient absorption spectra recorded at (a) 0 μs, (b) 40 μs, and (c) 140 μs after the pulse radiolysis of aqueous NaSCN (0.05 M) solution (N_2O saturated) containing SiO_2/Al_2O_3/Aucolloids ([Au] = 1 mM and $[SiO_2/Al_2O_3]$ = 0.04 M).

Surface complexation with $(SCN_2)^{\bullet -}$ radicals is also expected to dampen the surface plasmon band of gold nanoparticles. The plasmon absorption change associated with surface complexation cannot be resolved in the transient absorption studies if the complexing species has relatively larger absorption. Since the absorption of $(SCN)_2^{\bullet -}$ and $[Au\cdots(SCN)_2^{\bullet -}]$ species dominate the absorption in the visible (up to 600 nm), we were not able to see any bleaching of the surface plasmon band. However, a careful look at the spectra in Figure 2 indicates a dip in the region of 530 nm. (Note that this dip is not seen for the small size Au nanoparticles (2 nm diameter) that do not possess plasmon absorption (Figure 1 in Supporting Information).

These observations suggest that the transient (absorbance maximum at 390 nm) observed at longer times in Figure 2 results from the interaction between $(SCN)_2^{\bullet -}$ and the gold surface. The equilibrium (3) illustrates the formation of an associated complex between Au^0 and $(SCN)_2^{\bullet -}$ radicals.

$$Au^0 + (SCN)_2^{\bullet -} \rightleftarrows [Au^0\text{---}(SCN)_2^{\bullet -}] \qquad (3)$$

The complex ($[Au^0\text{---}(SCN)_2^{\bullet -}]$) formed during the initial interaction between gold surface and $(SCN)_2^{\bullet -}$ radicals can be in equilibrium with $[Au^0\text{---}(SCN)^\bullet]$ and SCN^-species (equilibrium 4).

$$[Au^0 \text{- - -} (SCN)_2^{\bullet -}] \rightleftarrows [Au^0 \text{- - -} (SCN)^\bullet] + SCN^- \qquad (4)$$

However, the presence of high SCN^- concentration makes the dissociation of $[Au^0\text{- - -}(SCN)_2^{\bullet -}]$ less likely. Moreover, we have not found any kinetic or spectral evidence for the formation of additional species during the decay of $(SCN)_2^{\bullet -}$. It may be interesting to note that the $^\bullet OH$ radical adduct of SCN^- has also been shown to have an absorption maximum at 390 nm.[46] We would like to refer to the thiocyanate radical complex with gold as $[Au^0\text{- - -}(SCN)_2^{\bullet -}]$ in following discussions.

In order to further evaluate the complexation process, we monitored the absorbance growth (390 nm) at different concentrations of SiO_2/Al_2O_3/Au nanoparticles. With increasing concentration of SiO_2/Al_2O_3/Au particles (expressed in terms of molecular concentration of gold, [Au]) we observed an increase in the absorption at 390 nm (Figure 3). Since the maximum absorbance (ΔA_{max}) at 390 nm is dependent on the concentration of the complex, one can employ the Benesi−Hildebrand method[47] to determine the apparent equilibrium constant. From the double reciprocal plot of $1/\Delta A_{max}$ versus 1/[Au] (inset of Figure 3), we obtain an apparent equilibrium

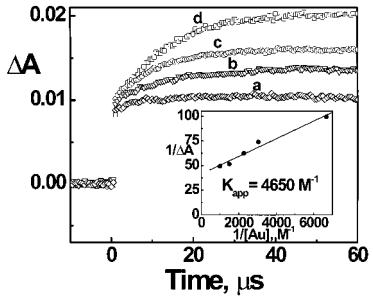

Figure 3. Growth of $[Au^0 - - -(SCN)_2^{\bullet -}]$ complex at different concentrations of $SiO_2/AlO_3/Au$ colloids. The absorption−time profiles at 390 nm were recorded following the pulse radiolysis of aqueous NaSCN (0.05 M) solution (N_2O saturated) containing gold colloids with the concentration of [Au] corresponding to (a) 0.15 mM, (b) 0.33 mM, (c) 0.44 mM, and (d) 1 mM. The inset shows the plot of $1/\Delta A_{max}$(390 nm) versus 1/[Au].

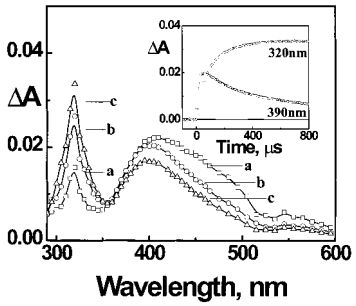

Figure 4. Transient absorption spectra recorded at (a) 140 μs, (b) 400 μs, and (c) 750 μs after the pulse radiolysis of aqueous NaSCN (0.05 M) solution (N_2O saturated) containing $SiO_2/Al_2O_3/Au$ colloids ([Au] = 1 mM). Inset shows the absorption−time profiles recorded at 390 and 320 nm.

constant of 4650 M^{-1} for the association between Au^0 and $(SCN)_2^{\bullet -}$. Such a high value of apparent equilibrium constant suggests that $(SCN)_2^{\bullet -}$ radicals are able to interact strongly with the gold surface.

It has been suggested that in some instances the colloidal metals behave like nonprecious metals.[48] For example, complexants having −SH, $-NH_2$, or −SCN functional groups readily interact with gold colloids and dampen the surface plasmon bands.[14] In another study, the strong adsorption of CS_2 to silver nanoclusters has been explained on the basis of simultaneous binding of the two sulfur atoms to the silver surface.[49] To the best of our knowledge, this is the first report that identifies significant spectral changes that arise from the complexation with short-lived radicals.

The pseudo-first-order rate constant of the formation of the complex was found to be dependent on the concentration of gold colloids. The bimolecular rate constant obtained from the linear dependence of the pseudo-first-order decay rate constant of $(SCN)_2^{\bullet -}$ radical on the gold colloid concentration was calculated to be 1.5×10^7 M^{-1} s^{-1}. This value of the bimolecular rate constant should be considered as an apparent value since we have employed molecular concentration of gold present in the $SiO_2/Al_2O_3/Au$ colloids. Since the actual particle concentration is at least 3 orders of magnitude less than the molecular gold concentration we expect the rate constant to be nearly diffusion-controlled.

The charge transfer complex, $[Au^0 - - -(SCN)_2^{\bullet -}]$, is relatively short-lived (lifetime of ~100 μs) as indicated by the absorption decay at 390 nm. The spectral changes that occur during the decay of $[Au^0 - - -(SCN)_2^{\bullet -}]$ are shown in Figure 4. Formation of a new transient with an absorbance maximum at 320 nm is

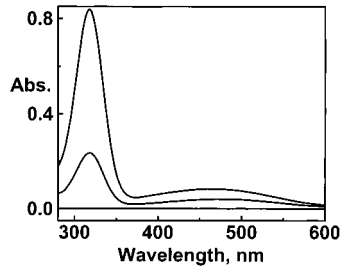

Figure 5. Absorption spectra recorded after the addition of $HAuCl_4$ solution to 0.5 M NaSCN in aqueous solution (N_2O) saturated. The concentrations of $[AuCl_4]^-$ were (a) 0 mM, (b) 1.2 mM, and (c) 2.1 mM.

apparent as the transient at 390 nm decreased. The inset shows the growth of the 320 nm transient and the corresponding decay of the 390 nm transient.

These results indicate that the $[Au^0 - - -(SCN)_2^{\bullet -}]$ complex undergoes chemical changes over a time period of 800 μs. The $(SCN)_2^{\bullet -}$ radical is a mild oxidant and is capable of inducing chemical changes following its complexation with gold nanoclusters.

$$[Au^0 - - -(SCN)_2^{\bullet -}] \rightarrow [Au^I(SCN)_2]^- \quad (5)$$

In order to establish the identity of this newly formed product (reaction 5) we employed an indirect approach of generating $[Au(SCN)_2]^-$ by the reduction of $[AuCl_4]^-$ with NaSCN. A few earlier studies[50−53] have presented a detailed account of ligand substitution of the $[AuCl_4]^-$ with SCN^- to produce $[Au(SCN)_4]^-$ species in aqueous solution. These studies also suggest that the $[Au(SCN)_4]^-$ ultimately undergoes reduction in the presence of excess SCN^- to produce an $[Au(SCN)_2]^-$ complex (reactions 6 and 7).

$$[AuCl_{4-n}(SCN)_n]^- + SCN^- \rightarrow [AuCl_{3-n}(SCN^-)_{n+1}]^- + Cl^- \quad (6)$$

$$[Au(SCN)_4]^- + 2SCN^- \rightarrow [Au(SCN)_2]^- + 2(SCN)_2^{\bullet -} \quad (7)$$

Addition of $[AuCl_4]^-$ to deaerated solution of concentrated NaSCN in the present experiment yielded the desired product, $[Au(SCN)_2]^-$, with characteristic absorption in the UV region (Figure 5). The complex $[Au(SCN)_2]^-$ was relatively stable in the deaerated aqueous solutions and was accessible for spectral characterizations. This complex which has an absorption maximum at 320 nm closely resembles the long time scale transient spectrum recorded in the pulse radiolysis experiment. The similarity in the spectral profiles of the two methods, viz., the reduction of Au^{3+} by SCN^- or the oxidation of Au^0 by $(SCN)_2^{\bullet -}$, confirms the identity of Au^I species (viz., $[Au(SCN)_2]^-$).

The pulse radiolysis results presented in this investigation demonstrate the ability of short-lived radicals such as $(SCN_2)^{\bullet -}$ to chemically interact with gold nanoparticles and induce oxidation of the gold surface. The spectral evolution of the Au^0 and $(SCN_2)^{\bullet -}$ complex as well as the oxidation product establishes the underlying chemistry of these surface bound radicals. Such chemical interactions have to be given serious consideration when employing metal nanoparticles in catalytic and biological applications that encounter mild oxidizing radicals.

Acknowledgment. We would like to thank Dr. Dan Meisel for helpful discussions. The work described herein was sup-

ported by the Office of the Basic Energy Sciences of the US Department of Energy. This is contribution No. 4257 from the Notre Dame Radiation Laboratory.

Supporting Information Available: Figures 1 and 2 showing the time-resolved transient spectra of the reaction of $(SCN)_2^{\bullet-}$ radicals with 2 nm diameter gold nanoparticles (prepared in the absence of SiO_2/Al_2O_3 core) in aqueous medium. This material is available free of charge via the Internet at http://pubs.acs.org.

References and Notes

(1) Hickman, J. J.; Ofer, D.; Laibinis, P. E.; Whitesides, G. M.; Wrighton, M. S. *Science* **1991**, *252*, 688.
(2) Chen, S.; Ingram, R. S.; Hostetler, M. J.; Pietron, J. J.; Murray, R. W.; Schaaff, T. G.; Khoury, J. T.; Alvarez, M. M.; Whetten, R. L. *Science* **1998**, *280*, 2098.
(3) Elghanian, R.; Storhoff, J. J.; Mucic, R. C.; Letsinger, R. L.; Mirkin, C. A. *Science* **1997**, *277*, 1078.
(4) Akiyama, T.; Imahori, H.; Ajawakom, A.; Sakata, Y. *Chem. Lett.* **1996**, 907.
(5) Liz-Marzán, L. M.; Giersig, M.; Mulvaney, P. *Langmuir* **1996**, *12*, 4329.
(6) Mulvaney, P. Spectroscopy of metal colloids. Some comparisons with semiconductor colloids. In *Semiconductor Nanoclusters—Physical, Chemical and Catalytic Aspects.*; Kamat, P. V., Meisel, D., Eds.; Elsevier Science: Amsterdam, 1997; p 99.
(7) Porter, L. A.; Ji, D.; Westcott, S. L.; Graupe, M.; Czernuszewicz, R. S.; Halas, N. J. *Langmuir* **1998**, *14*, 7378.
(8) Shanghavi, B.; Kamat, P. V. *J. Phys. Chem. B* **1997**, *101*, 7675.
(9) Fujiwara, H.; Yanagida, S.; Kamat, P. V. *J. Phys. Chem. B* **1999**, *103*, 2589.
(10) Templeton, A. C.; Cliffel, D. E.; Murray, R. W. *J. Am. Chem. Soc.* **1999**, *121*, 7081.
(11) Fitzmaurice, D.; Rao, S. N.; Preece, J. A.; Stoddart, J. F.; Wenger, S.; Zaccheroni, N. *Angew. Chem., Int. Ed. Engl.* **1999**, *38*, 1147.
(12) Makarova, O. V.; Ostafin, A. E.; Miyoshi, H.; Norris, J. R.; Meisel, D. *J. Phys. Chem. B* **1999**, *103*, 9080.
(13) George Thomas, K.; Kamat, P. V. *J. Am. Chem. Soc.* **2000**, *122*, 2655.
(14) Linnert, T.; Mulvaney, P.; Henglein, A. *J. Phys. Chem.* **1993**, *97*, 679.
(15) Gutierrez, M.; Henglein, A. *J. Phys. Chem.* **1993**, *97*, 11368.
(16) Kreibig, U.; Vollmer, M. *Optical Properties of Metal Clusters*; Springer: Berlin, 1995.
(17) Kreibig, U.; Gartz, M.; Hilger, A.; Hovel, H. Mie-plasmon spectroscopy: A tool of surface science. In *Fine Particles Science and Technology*; Pelizzatti, E., Ed.; Kulwer Academic Publishers: Boston, MA, 1996; p 499.
(18) Link, S.; El-Sayed, M. A. *J. Phys. Chem. B* **1999**, *103*, 8410.
(19) Heller, A.; Aharon, S. E.; Bonner, W. A.; Miller, B. *J. Am. Chem. Soc.* **1982**, *104*, 6942.
(20) Nosaka, Y.; Norimatsu, K.; Miyama, H. *Chem. Phys. Lett.* **1984**, *106*, 128.
(21) Anderson, M. L.; Morris, C. A.; Stroud, R. M. *Langmuir* **1999**, *15*, 674.
(22) Averitt, R. D.; Westcott, S. L.; Halas, N. J. *J. Opt. Soc. Am. B. Opt. Phys.* **1999**, *16*, 1814.
(23) Averitt, R. D.; Westcott, S. L.; Halas, N. J. *J. Opt. Soc. Am. B. Opt. Phys.* **1999**, *16*, 1824.
(24) Oldenburg, S. J.; Jackson, J. B.; Westcott, S. L.; Halas, N. J. *Appl. Phys. Lett.* **1999**, *75*, 2897.
(25) Westcott, S. L.; Oldenburg, S. J.; Lee, T. R.; Halas, N. J. *Chem. Phys. Lett.* **1999**, *300*, 651.
(26) Meisel, D.; Mulac, W. A.; Matheson, M. S. *J. Phys. Chem.* **1981**, *85*, 179.
(27) Matheson, M. S.; Lee, P. C.; Meisel, D.; Pelizzetti, E. *J. Phys. Chem.* **1983**, *87*, 394.
(28) Nahor, G. S.; Neta, P.; Hambright, P.; Thompson, A. N. J.; Harriman, A. *J. Phys. Chem.* **1989**, *93*, 6181.
(29) Henglein, A. *J. Phys. Chem.* **1993**, *97*, 5457.
(30) de Cointet, C.; Mostafavi, M.; Khatouri, J.; Belloni, J. *J. Phys. Chem. B* **1997**, *101*, 3512.
(31) Belloni, J. Photocatalytic aspects of silver photography. In *Homogeneous Photocatalysis*; Chanon, M., Ed.; John Wiley & Sons: New York, 1997; p 170.
(32) Baschong, W.; Lucocq, J. M.; Roth, J. *Histochemistry* **1985**, *83*, 409.
(33) Chandrasekharan, N.; Kamat, P. V.; Hu, J.; Jones II, G. *J. Phys. Chem.* **2000**, *104*, 11103.
(34) Turkevich, J.; Stevenson, P. L.; Hillier, J. *Discuss. Faraday Soc.* **1951**, *11*, 55.
(35) Henglein, A. *Ber. Bunsen-Ges. Phys. Chem.* **1982**, *86*, 301.
(36) Frank, A. J.; Willner, I.; Goren, Z.; Degani, Y. *J. Am. Chem. Soc.* **1987**, *109*, 3568.
(37) Oldenburg, S. J.; Averitt, R. D.; Westcott, S. L.; Halas, N. J. *Chem. Phys. Lett.* **1998**, *288*, 243.
(38) Kamat, P. V.; Ford, W. E. *J. Phys. Chem.* **1989**, *93*, 1405.
(39) Ford, W. E.; Kamat, P. V. *J. Phys. Chem.* **1989**, *93*, 6423.
(40) Averitt, R. D.; Westcott, S. L.; Oldenburg, S. J.; Lee, T. R.; Halas, N. J. *Langmuir* **1998**, *14*, 5396.
(41) Ocana, M.; Hsu, W. P.; Matijevic, E. *Langmuir* **1991**, *7*, 2911.
(42) Giesche, H.; Matijevic, E. *J. Mater. Res.* **1994**, *9*, 436.
(43) Hardikar, V.; Matijevic, E. *J. Colloid Interface Sci* **2000**, *221*, 133.
(44) Henglein, A.; Meisel, D. *Langmuir* **1998**, *14*, 7392.
(45) Persson, B. N. J. *Phys. Rev. B* **1989**, *39*, 8220.
(46) Behar, D.; Bevan, P. L. T.; Scholes, G. *J. Phys. Chem.* **1972**, *76*, 1537.
(47) Benesi, H. A.; Hildebrand, J. H. *J. Am. Chem. Soc.* **1949**, *71*, 2703.
(48) Henglein, A. *Chem. Mater.* **1998**, *10*, 444.
(49) Henglein, A.; Meisel, D. *J. Phys. Chem. B* **1998**, *102*, 8364.
(50) Hall, A. J.; Satchell, D. P. N. *J. Chem. Soc. Chem. Commun.* **1976**, 163.
(51) Hall, A. J.; Satchell, D. P. N. *J. Chem. Soc., Dalton Trans.* **1977**, 1403.
(52) Elding, L. I.; Groning, A. B.; Groning, O. *J. Chem. Soc., Dalton Trans.* **1981**, 1093.
(53) Elmroth, S. K. C.; Elding, L. I. *Inorg. Chem.* **1996**, *35*, 2337.